

Rapid Oxidation of Skin Oil by Ozone

Shouming Zhou, Matthew W. Forbes, Yasmine Katrib, Jonathan P.D. Abbatt

Version Post-print/Accepted Manuscript

Citation (published version) Zhou, S., Forbes, M.W., Katrib, Y., Abbatt, J.P.D., 2016. Rapid Oxidation of Skin Oil by Ozone. *Environ. Sci. Technol. Lett.* 3, 170–174. <https://doi.org/10.1021/acs.estlett.6b00086>.

Copyright / License This document is the Accepted Manuscript version of a Published Work that appeared in final form in *Environmental Science & Technology Letters*, copyright © American Chemical Society after peer review and technical editing by the publisher. To access the final edited and published work see <https://pubs.acs.org/doi/10.1021/acs.estlett.6b00086>.

How to cite TSpace items

Always cite the published version, so the author(s) will receive recognition through services that track citation counts, e.g. Scopus. If you need to cite the page number of the **author manuscript from TSpace** because you cannot access the published version, then cite the TSpace version **in addition to** the published version using the permanent URI (handle) found on the record page.

This article was made openly accessible by U of T Faculty.
Please [tell us](#) how this access benefits you. Your story matters.

1
2
3
4
5
6
7 **Rapid Oxidation of Skin Oil by Ozone**
8
9

10
11 Shouming Zhou*, Matthew W. Forbes, Yasmine Katrib, Jonathan P.D. Abbatt
12 Department of Chemistry, University of Toronto
13 80 St. George St.
14 Toronto, ON, M5S 3H6, Canada
15

16 * - to whom correspondence should be addressed (Tel. +1-416-946-7359; Fax. +1-416-946-
17 7359; email: szhou@chem.utoronto.ca)
18
19
20
21

22 **Abstract**

23 The reaction of gas-phase ozone with human skin oil has been studied at room temperature. Skin
24 oil was exposed to ozone at mixing ratios similar to those in the ambient environment, and then
25 analyzed for condensed-phase products using Direct Analysis in Real Time-Mass Spectrometry
26 (DART-MS). Prior to ozone exposure, skin oil gives rise to prominent mass spectral signals
27 indicative of highly unsaturated alkenes, sterols, triglycerides, long chain fatty acids, pyroglutamic
28 acid, and probably waxy esters. Upon oxidation with 50 ppb ozone for 90 minutes, there is rapid
29 loss of alkene, fatty acid, and triglyceride signals resulting from efficient multi-phase ozonolysis.
30 Oxygenated products including a variety of carboxylic acids are identified via studies with pure
31 compounds present in skin oil, i.e. squalene, cholesterol and triolein. The chemistry is rapid,
32 occurring on timescales of tens of minutes, implying that these highly oxygenated reaction
33 products are always present on human skin both indoors and outdoors.
34
35
36
37

38

39 **Introduction**

40 A major advance in our understanding of the chemistry of the indoor environment is recognition
41 of the role of human occupants.¹ One class of impacts arises from multi-phase chemistry,
42 especially skin oils present either on human subjects or flakes/oils deposited in indoor
43 environments.²⁻⁴ Gas-phase products arising from the ozonolysis of carbon-carbon double bonds
44 within skin lipids have been identified.³⁻⁶ As well, the rate of ozone deposition in indoor
45 environments and ensuing chemistry depends on the level of human occupancy, where reactive
46 loss of ozone can occur directly either on humans, their soiled clothes or skin materials that they
47 deposit.^{4,6-12}

48
49 The multi-phase reactions of ozone with condensed-phase unsaturated organics occur
50 efficiently.^{13,14} Typical functional groups formed from ozone reacting with an alkene include
51 carbonyls, carboxyls, hydroxyl ketones and potentially hydroxyhydroperoxides. To better
52 understand the nature of chemistry occurring indoors arising from skin oil chemistry, experiments
53 have examined the oxidation of squalene with ozone.¹⁵⁻¹⁹ The kinetics are fast, with reactive uptake
54 coefficients of 10^{-5} to 10^{-3} . Both gas- and condensed-phase products have been identified,
55 including carbonyls, acids, peroxides and ethers.^{16,17,19} The condensed-phase products are more
56 hydrophilic and redox-active than squalene.¹⁸ As well, the oxidation products of fabrics soiled with
57 squalene have been studied under ambient conditions.²⁰

58
59 Many studies have been conducted on the chemical composition of skin surface lipids, with major
60 components including long-chain alkenes (e.g. squalene, 10% by mass), saturated and unsaturated
61 triglycerides (25%), fatty acid esters (22%), long-chain saturated and unsaturated fatty acids
62 (25%), sterols (2%) and natural moisturizing agents (a few percent).²¹⁻²⁶ We do not attempt to
63 reproduce these compositional studies. Rather, our goals in this work are to use DART-MS²⁷ to: i)
64 analyze the change in the composition of skin oil upon exposure to ozone, identifying the species
65 that react most efficiently and the oxidation products that remain in the condensed phase, and ii)
66 assess the oxidative transformation timescales of key components at an environmentally relevant
67 ozone mixing ratio. The motivations are to: i) provide kinetic information to interpret rates of
68 ozone loss in inhabited indoor spaces, ii) identify components of skin oil that are unreactive with

69 ozone that could be used to track human input to surfaces, and iii) identify condensed-phase
70 oxidation products to understand the factors impacting the composition of indoor surfaces.
71 Condensed-phase products have not been previously identified upon exposure of skin oil to ozone,
72 even though this chemistry will be occurring in both indoor and outdoor environments.

73

74 **Experimental**

75 Experiments were conducted using DART-MS analysis.²⁸ Samples are deposited onto the lower 5
76 mm of 1.6 mm-o.d. glass capillaries mounted in a Teflon holder. For skin oil, participants
77 reproducibly touched the tip of the capillary with their fingers. Prior to applying the skin oil, the
78 participants had not used personal care products for two days. They washed their hands with soap
79 and water, and then rubbed hands over face and arms. Although we present the oxidation mass
80 spectra of one specific male participant's skin oil, we also examined the spectra of three other male
81 participants. The major spectral features were observed in all four skin oil samples although, as
82 expected, there were variations in relative intensities of peaks from participant to participant, and
83 from day-to-day; however, this variability is not relevant to the kinetics results. Rather it is the
84 variability of the measurements amongst a set of coated tubes (commonly $\pm 20\%$ for 10 replicates)
85 that impacts the precision of the kinetics. The pure substances used as references in the product
86 analysis (100 ng) were applied as 1 μL dilute solutions in dichloromethane to the tip of the glass
87 capillary, after which the solvent evaporated. The relative standard deviation of major peaks was
88 also $\pm 20\%$. We believe that this analytical method is largely sensitive to the free molecules present
89 in the sebum (i.e. fatty secretions from the sebaceous glands) rather than lipid materials that are
90 physically bound in the epidermis.

91

92 Ozone exposure was conducted at 295 ± 3 K by placing the mounted capillaries in a glass flow tube
93 through which ozone mixed in air flowed with a residence time of ~ 40 s.²⁸ We performed control
94 experiments whereby both pure component and skin oil samples were analyzed for time periods
95 up to 90 minutes with no ozone, and we observed no loss of signal due to volatilization beyond
96 the variability stated above. After ozone/air exposure the samples were stored in a desiccator where
97 a small flow of nitrogen was added to avoid contamination from room air.

98

99 DART-MS analysis was performed by passing the coated capillaries in front of the ion source
100 (IonSense Inc.) on a motorized rail at a speed of 0.3 mm/second. The DART source was held at
101 500°C, resulting in (280±20)°C at the capillary sample, and used a helium flow of 3.0 liter/min.
102 Ambient air from the lab was present in the source region. Mass spectra were measured with a
103 JMS-T100LC time-of-flight mass spectrometer (JEOL USA Inc.) having mass resolution of
104 approximately 6000 at a mass-to-charge ratio (m/z) 600.

105

106 **Results and Discussion**

107 1. Skin oil characterization

108 A typical positive ion mass spectrum of skin oil is shown as the red trace in Figure 1a which has
109 four noteworthy features. First, two of the strongest peaks are due to squalene (Molecular Weight,
110 MW = 410.4 amu for the C12 isomer) with the first peak (m/z 411.4) arising from protonation in
111 the ion source and the second (m/z 428.4) due to addition of ammonium arising from trace
112 ammonia in the lab air. Control experiments with pure squalene confirm this assignment (Figure
113 S1). Second, we attribute the strong peak at m/z 369.3 to skin lipid sterols, such as cholesterol and
114 lathosterol.²⁵ Control experiments (Figure S2) demonstrate that cholesterol is detected at m/z 369.3
115 following loss of water from protonated cholesterol (m/z 387.3), a common fragmentation for
116 protonated alcohols. This peak in the skin oil may also arise from sterol esters.²⁹ Third, there is a
117 cluster of peaks from just below m/z 800 to 1000 (see Table S1). These peaks likely arise from
118 triglycerides, with roughly equal abundance in skin lipids of the unsaturated and saturated forms.²⁵
119 The unsaturated forms have hydrocarbon chains 14-24 carbon atoms long (i.e. MW=700-1100
120 amu). Results from a control experiment with a pure C18 mono-unsaturated triglyceride, triolein
121 (MW = 884.8 amu for C12 isomer), are shown in Figure S3. The DART-MS spectrum shows
122 intensity for ammoniated triolein (m/z 902.7) and a fragment ion of protonated triolein (m/z 603.5)
123 following the loss of a C18 mono-unsaturated fatty acid (MW = 282.4 amu). The fourth cluster of
124 peaks in the positive ion mass spectrum, i.e. those between m/z 450 and 600 (Table S1), may arise
125 from the triglycerides or waxy esters (typically mono- and di-esters with 10 to 20 carbon chains,
126 MW = 450 to 600).²⁵ These peak assignments are in agreement with the DART-MS literature.²⁹

127

128 A fifth important class of compounds, the long-chain fatty acids, is observed with three large peaks
129 in the negative ion spectrum at m/z 253.2, 255.2 and 281.2 (Figure 1b and Table S1). These likely

130 correspond to the most abundant fatty acids in skin lipids, cis-hexadec-6-enoic acid (MW=254.2
131 amu for C12 isomer), palmitic acid (MW=256.2 amu for C12 isomer), and cis-octadec-8-enoic
132 acid (MW=282.3 amu for C12 isomer).²⁵ Organic acids are detected by proton abstraction in
133 negative ion mode DART-MS, i.e. at $[M-H]^+$.

134
135 The most prominent peak in the negative ion spectrum is observed at m/z 128.0. Control
136 experiments show that glutamic acid and pyroglutamic acid contribute to this mass (Figure S4).
137 Using HPLC-MS analysis (see SI-Text, Figures S5, S6), we established that this peak is mainly
138 due to pyroglutamic acid, a natural moisturizing substance present at the 1% level in the human
139 epidermis.^{21,23,26}

140

141 2. Oxidation kinetics of skin oil and common skin oil materials

142 The blue traces in Figure 1a and 1b correspond to an ozone exposure of 50 ppb for 90 minutes.
143 There is loss of intensity in a large number of peaks and formation of intensity at others. The
144 squalene peaks lose their prominence entirely, the triglyceride peaks are significantly depleted, as
145 are peaks from m/z 450 to 600 (see Table S1). The intensity of the sterol peak at m/z 369.3 is
146 reduced slightly but decreases by 50% when exposed to 300 ppb ozone for 45 minutes (data not
147 shown). In the negative ion mode, the peaks due to the fatty acids all decrease substantially with
148 the peak at m/z 255.2 (likely palmitic acid) decreasing to ~60% of its starting value and those at
149 m/z 253.2 and 281.2 decreasing more than 70%.

150
151 Squalene is an unsaturated compound that reacts rapidly with ozone.¹⁶⁻¹⁸ A decay plot
152 demonstrates the rapid kinetics of pure squalene heterogeneous ozonolysis, with an e-folding
153 lifetime of 10 minutes with 50 ppb ozone (Figure 2c). Triolein, the oleic acid tri-ester of glycerol,
154 shows similar reactivity (Figure 2d). These liquids react more rapidly than pure cholesterol which
155 is a solid at ambient temperature (Figure 2b). Although cholesterol is known to react with
156 ozone,^{30,31} its phase may be the reason for the lower reactivity.

157
158 The sterol peak (m/z 369.3) shows similar loss kinetics to that of pure cholesterol (Figure 2b), with
159 a small decay at early times. By comparison, the peaks due to squalene (m/z 411.4) and cis-
160 hexadec-6-enoic acid (m/z 253.2) show more reactivity, with some saturation of the reactivity at

161 long times (Figure 2d). This is likely due to burial of some of the molecules in the skin oil matrix,
162 limiting exposure to ozone at the surface. For probably the same reason, the squalene signal does
163 not decay as rapidly as when present as a pure compound, with an e-fold lifetime of about 30
164 minutes (Figure 2c). The peak assigned to palmitic acid (m/z 255.2) also exhibits initial decay and
165 the same plateau in the signal at long times (Figure 2d). Since palmitic acid does not react directly
166 with ozone, this may be due to reaction with reactive intermediates such as Criegee biradicals.
167 Whether other species also react with intermediates of this type is not known.

168
169 The peak due to pyroglutamic acid does not decay with ozone (Figure 2a) consistent with it not
170 containing a carbon-carbon double bond. This chemical may be a convenient tracer of human skin
171 oil contamination in indoor environments, given its relatively high abundance and low reactivity
172 with ozone.

173
174 3. Products formed from oxidation of skin oil and common skin oil materials

175 The pure substance experiments help to interpret the oxidation products. Prominent products from
176 squalene are observed only in the negative ion mode. The dominant peaks at m/z 115.0 and 117.0
177 are consistent with levulinate and succinate anions, respectively (Figure S1). The corresponding
178 acids are reaction end products, formed via successive ozonolysis reactions at the multiple carbon-
179 carbon double bonds in squalene, yielding at each step carbonyl and carboxylic acid functional
180 groups upon bond breakage. These products are present in the skin oil oxidation experiment, as
181 seen in the inset in Figure 1b. Other dicarboxylic acids, including adipic acid and suberic acid,
182 arising from oxidation of the most common unsaturated acids, cis-hexadec-6-enoic acid and cis-
183 octadec-8-enoic acid, respectively, are also observed at m/z 145.0 and 173.1. We note that a study
184 of squalene oxidation indicated substantial product formation at high molecular weights.¹⁹ The
185 positive ion DART-MS spectra of squalene similarly show the formation of high MW products
186 upon ozone oxidation (>450 amu) (Figure S1).

187
188 Although cholesterol reacts slowly, the products formed (m/z 385.3, 401.3, 417.3 in the positive
189 ion spectrum and m/z 433.3 in the negative ion spectrum, Figure S2) arise from addition of 1, 2 or
190 3 oxygen atoms, respectively, to its carbon-carbon double bond. For example, the three-oxygen
191 product, i.e. m/z 417.3 in the positive ion spectrum, could arise from ozonolysis of the carbon-

192 carbon double bond into an aldehyde and carboxylic acid. Given the small decay of cholesterol, it
193 is not possible to identify these product peaks in the skin oil spectrum.

194
195 The positive ion DART-MS spectra of triolein before and after exposure are shown in Figure S3.
196 It is not surprising that, with three double bonds, triolein yields a large number of ozonolysis
197 products that are observed from m/z 450-800. A common feature is that they all have molecular
198 weights lower than the parent triolein molecule, indicating that ozonolysis leads to cleavage of an
199 alkyl chain and formation of a distribution of smaller products. These observations are consistent
200 with those made from the skin oil experiments in which high MW skin oil components (m/z 750-
201 to 1000) disappeared after ozone reaction whereas lower MW species from m/z 450-800 formed.
202 The most intense peak in the negative ion mass spectrum (m/z 157.1) is consistent with the
203 formation of nonanoic acid, a low volatility product arising from ozonolysis of the oleate chain in
204 triolein.

205
206 To illustrate the kinetics of product formation, the time-dependent signals of oxidation products
207 from squalene and cis-hexadec-6-enoic acid are shown in Figure 2c,d, along with a likely oxidation
208 product at $m/z(-)$ 585.3 from unsaturated triglycerides. This oxidation product was observed from
209 triolein (Figure S3).

210
211 4. Environmental Significance
212 This investigation is the first mass spectrometry study of the chemical changes occurring in the
213 condensed phase when skin oil is exposed to ozone. By focussing on the condensed phase products,
214 this work complements earlier studies that addressed the gas-phase products formed when ozone
215 interacts with human lipid materials containing species such as squalene.⁴

216
217 Driven by the unsaturated skin oil components present, the oxidative transformation is rapid as
218 seen by the significant change observed in the DART-MS spectrum after 90 minutes exposure to
219 50 ppb ozone. Specifically, squalene and the unsaturated fatty acids in skin oil have an oxidation
220 timescale on the order of tens of minutes at this ozone mixing ratio, a common outdoor value
221 during smog episodes; this lifetime will be longer indoors which typically have ozone levels 0.2
222 to 0.8 of those outdoors.³² We note that given the amount of time spent indoors, human ozone

223 exposure is frequently dominated by indoor exposure.³² The values used here, i.e. 75 ppb·hours,
224 are environmentally relevant being equivalent to one hour outdoors at 75 ppb ozone or 7.5 hours
225 indoors at 10 ppb. There is evidence for the formation of a suite of highly oxygenated species,
226 composed of carboxylic acids such as succinic acid, levulinic acid, higher dicarboxylic acids, and
227 highly functionalized species. One species, pyroglutamic acid, is not reactive with ozone which
228 may make it useful as a tracer of human contamination indoors.

229
230 These results imply that the oils covering human skin and those deposited to indoor surfaces are
231 being continually oxidized under ambient conditions, with a mixture of both endogenous
232 components alongside their heterogeneous oxidation products. The oxidation products are less
233 reactive than the precursors, thus making the surfaces less reactive than a fresh skin oil surface.
234 As well, the impacts of the observed loss kinetics of the many skin oil species could be related to
235 ozone loss indoors, using a coupled indoor air – multiphase chemistry model. It will be important
236 to determine the toxicological properties of the oxidation products given earlier work that has
237 indicated that squalene oxidation gives rise to redox-active condensed-phase materials and gas-
238 phase products that are irritants.^{18,33}

239
240 **Supporting Information:**
241 Mass spectra (with and without ozone) of squalene, cholesterol, triolein and their ozonolysis
242 products obtained by DART-MS (Figure S1-S3); mass spectra of glutamic and pyroglutamic acids
243 obtained by DART-MS (Figure S4) and ESI-MS (Figure S5); extracted ion chromatograms of
244 HPLC-MS analysis of glutamic and pyroglutamic acids (Figure S6); lists of major peaks of skin
245 oil, squalene, cholesterol and triolein and their ozonolysis products (Table S1-S4); description of
246 the HPLC-MS analysis (SI-Text).

247
248 **Acknowledgements**
249 This work was supported by the Sloan Foundation, Grant G2013-10-05.

250
251 **References**
252 (1) Weschler, C. J., Roles of the Human Occupant in Indoor Chemistry, *Indoor Air*
253 **2016**, *26*, 6-24.

- 254 (2) Clark, R. P.; Shirley, S. G., Identification of Skin in Airborne Particulate Matter,
255 *Nature* **1973**, *246*, 39-40.
- 256 (3) Pandrangi, L. S.; Morrison, G. C., Ozone Interactions with Human Hair: Ozone
257 Uptake Rates and Product Formation *Atmos. Environ.* **2008**, *42*, 5079-5089.
- 258 (4) Wisthaler, A.; Weschler, C. J., Reactions of Ozone with Human Skin Lipids:
259 Sources of Carbonyls, Dicarbonyls, and Hydroxycarbonyls in Indoor Air, *Proc. Natl. Acad. Sci.*
260 *USA* **2009**, *107*, 6568-6575.
- 261 (5) Wisthaler, A.; Tamas, G.; Wyon, D. P.; Strom-Tejsen, P.; Space, D.; Beauchamp,
262 J.; Hansel, A.; Mark, T. D.; Weschler, C. J., Products of Ozone-initiated Chemistry in a Simulated
263 Aircraft Environment, *Environ. Sci. Technol.* **2005**, *39*, 4823-4832.
- 264 (6) Coleman, B. K.; Destailats, H.; Hodgson, A. T.; Nazaroff, W. W., Ozone
265 Consumption and Volatile Byproduct Formation from Surface Reactions with Aircraft Cabin
266 Materials and Clothing Fabrics, *Atmos. Environ.* **2008**, *42*, 642-654.
- 267 (7) Fischer, A.; Ljungstrom, E.; Langer, S., Ozone Removal by Occupants in a
268 Classroom, *Atmos. Environ.* **2013**, *81*, 11-17.
- 269 (8) Tamas, G.; Weschler, C. J.; Bako-Biro, Z.; Wyon, D. P.; Strom-Tejsen, P., Factors
270 Affecting Ozone Removal Rates in a Simulated Aircraft Cabin Environment, *Atmos. Environ.*
271 **2006**, *40*, 6122-6133.
- 272 (9) Rim, D.; Novoselec, A.; Morrison, G., The Influence of Chemical Interactions at
273 the Human Surface on Breathing Zone Levels of Reactants and Products, *Indoor Air* **2009**, *19*,
274 324-334.
- 275 (10) Rai, A. C.; Guo, B.; Lin, C. H.; Zhang, J. S.; Pei, J. J.; Chen, Q. Y., Ozone Reaction
276 with Clothing and Its Initiated Particle Generation in an Environmental Chamber, *Atmos. Environ.*
277 **2013**, *77*, 885-892.
- 278 (11) Fadeyi, M. O.; Weschler, C. J.; Tham, K. W.; Wu, W. Y.; Sultan, Z. M., Impact of
279 Human Presence on Secondary Organic Aerosols Derived from Ozone-Initiated Chemistry in a
280 Simulated Office Environment, *Environ. Sci. Technol.* **2013**, *47*, 3933-3941.
- 281 (12) Weschler, C. J.; Wisthaler, A.; Cowlin, S.; Tamas, G.; Strom-Tejsen, P.; Hodgson,
282 A. T.; Destailats, H.; Herrington, J.; Zhang, J. J.; Nazaroff, W. W., Ozone-initiated Chemistry in
283 an Occupied Simulated Aircraft Cabin, *Environ. Sci. Technol.* **2007**, *41*, 6177-6184.
- 284 (13) Kolb, C. E.; Cox, R. A.; Abbatt, J. P. D.; Ammann, M.; Davis, E. J.; Donaldson, D.
285 J.; Garrett, B. C.; George, C.; Griffiths, P. T.; Hanson, D. R.; Kulmala, M.; McFiggans, G.; Poschl,
286 U.; Riipinen, I.; Rossi, M. J.; Rudich, Y.; Wagner, P. E.; Winkler, P. M.; Worsnop, D. R.; O' Dowd,
287 C. D., An Overview of Current Issues in the Uptake of Atmospheric Trace Gases by Aerosols and
288 Clouds, *Atmos. Chem. Phys.* **2010**, *10*, 10561-10605.
- 289 (14) Abbatt, J. P. D.; Lee, A. K. Y.; Thornton, J. A. Quantifying Trace Gas Uptake to
290 Tropospheric Aerosol: Recent Advances and Remaining Challenges, *Chem. Soc. Rev.* **2012**, *41*,
291 6555-6581.
- 292 (15) Fruekilde, P.; Hjorth, J.; Jensen, N. R.; Kotzias, D.; Larsen, B., Ozonolysis at
293 Vegetation Surfaces: A Source of Acetone, 4-oxopentanal, 6-methyl-5-hepten-2-one, and Geranyl
294 Acetone in the Troposphere, *Atmos. Environ.* **1998**, *32*, 1893-1902.
- 295 (16) Wells, J. R.; Morrison, G. C.; Coleman, B. K. Kinetics and Reaction Products of
296 Ozone and Surface-bound Squalene, *J. ASTM Int.* **2008**, *5*, 1-12.
- 297 (17) Petrick, L.; Dubowski, Y., Heterogeneous Oxidation of Squalene Film by Ozone
298 Under Various Indoor Conditions, *Indoor Air* **2009**, *19*, 381-391.

299 (18) Fu, D.; Leng, C. B.; Kelley, J.; Zeng, G.; Zhang, Y. H.; Liu, Y., ATR-IR Study of
300 Ozone Initiated Heterogeneous Oxidation of Squalene in an Indoor Environment, *Environ. Sci.*
301 *Technol.* **2013**, *47*, 10611-10618.

302 (19) Fooshee, D. R.; Aiona, P. K.; Laskin, A.; Laskin, J.; Nizkorodov, S. A.; Baldi, P.
303 F., Atmospheric Oxidation of Squalene: Molecular Study Using COBRA Modeling and High-
304 Resolution Mass Spectrometry, *Environ. Sci. Technol.* **2015**, *49*, 13304-13313.

305 (20) Park, F. K. C.; Obendorf, S. K., Chemical Changes in Unsaturated Oils upon Aging
306 and Subsequent Effects on Fabric Yellowing and Soil Removal, *J. Am. Oil Chem. Soc.* **1994**, *71*,
307 17-30.

308 (21) Laden, K.; Sptizer, R., Identification of a Natural Moisturizing Agent in Skin, *J.*
309 *Soc. Cosmet. Chem.* **1967**, *18*, 351-360.

310 (22) Pochi, P. E.; Downing, D. T.; Strauss, J. S., Sebaceous Gland Response in Man to
311 Prolonged Total Caloric Deprivation, *J. Invest. Dermatol.* **1970**, *55*, 303-318.

312 (23) Marstein, S.; Jellum, E.; Eldjarn, L., The Concentration of Pyroglutamic Acid (2-
313 pyrrolidone-5-carboxylic Acid) in Normal and Psoriatic Epidermis, Determined on a Microgram
314 Scale by Gas-Chromatography, *Clin. Chim. Acta* **1973**, *49*, 389-395.

315 (24) Downing, D. T.; Strauss, J. S., Synthesis and Composition of Surface Lipids of
316 Human Skin, *J. Invest. Dermat.* **1974**, *62*, 228-244.

317 (25) Nicolaides, N., Skin Lipids - Their Biochemical Uniqueness, *Science* **1974**, *186*,
318 19-26.

319 (26) Rawlings, A. V.; Scott, I. R.; Harding, C. R.; Bowser, P. A., Stratum-corneum
320 Moisturization at the Molecular-level, *J. Invest. Dermat.* **1994**, *103*, 731-740.

321 (27) Cody, R. B.; Laramie, J. A.; Durst, H. D., Versatile New Ion Source for the
322 Analysis of Materials in Open Air Under Ambient Conditions, *Anal. Chem.* **2005**, *77*, 2297-2302.

323 (28) Zhou, S. M.; Forbes, M. W.; Abbatt, J. P. D., Application of Direct Analysis in Real
324 Time-Mass Spectrometry (DART-MS) to the Study of Gas-Surface Heterogeneous Reactions:
325 Focus on Ozone and PAHs, *Anal. Chem.* **2015**, *87*, 4733-4740.

326 (29) Mess, A.; Enthaler, B.; Fischer, M.; Rapp, C.; Pruns, J. K.; Vietzke, J. P., A Novel
327 Sampling Method for Identification of Endogenous Skin Surface Compounds by Use of DART-
328 MS and MALDI-MS, *Talanta* **2013**, *103*, 398-402.

329 (30) Gumulka, J.; Smith, L. L., Ozonation of Cholesterol, *J. Am. Chem. Soc.* **1983**, *105*,
330 1972-1979.

331 (31) Dreyfus, M. A.; Tolocka, M. P.; Dodds, S. M.; Dykins, J.; Johnston, M. V.,
332 Cholesterol Ozonolysis: Kinetics, Mechanism, and Oligomer Products, *J. Phys. Chem. A* **2005**,
333 *109*, 6242-6248.

334 (32) Weschler, C. J.; Shields, H. C.; Naik, D. V., Indoor Air Exposures, *I. Air Waste*
335 *Manag. Assoc.* **1989**, *39*, 1562-1568.

336 (33) Anderson, S. E.; Franko, J.; Jackson, L. G.; Wells, J. R.; Ham, J. E.; Meade, B. J.,
337 Irritancy and Allergic Responses Induced by Exposure to the Indoor Air Chemical 4-Oxopentanal,
338 *Toxicol. Sci.* **2012**, *127*, 371-381.

339
340
341
342
343

Supporting Information

Rapid Oxidation of Skin Oil by Ozone

Shouming Zhou*, Matthew W. Forbes, Yasmine Katrib, Jonathan P.D. Abbatt
Department of Chemistry, University of Toronto
80 St. George St.
Toronto, ON, M5S 3H6, Canada

* - to whom correspondence should be addressed (Tel. +1-416-946-7359; Fax. +1-416-946-7359; email: szhou@chem.utoronto.ca)

Summary (9 pages; 6 figures; 4 tables)

This supporting information contains: Mass spectra (with and without ozone) of squalene, cholesterol, triolein and their ozonolysis products obtained by DART-MS (Figure S1-S3); mass spectra of glutamic and pyroglutamic acids obtained by DART-MS (Figure S4) and ESI-MS (Figure S5); extracted ion chromatograms of HPLC-MS analysis of glutamic and pyroglutamic acids (Figure S6); lists of major peaks of skin oil, squalene, cholesterol and triolein and their ozonolysis products (Table S1-S4); description of the HPLC-MS analysis (SI-Text).

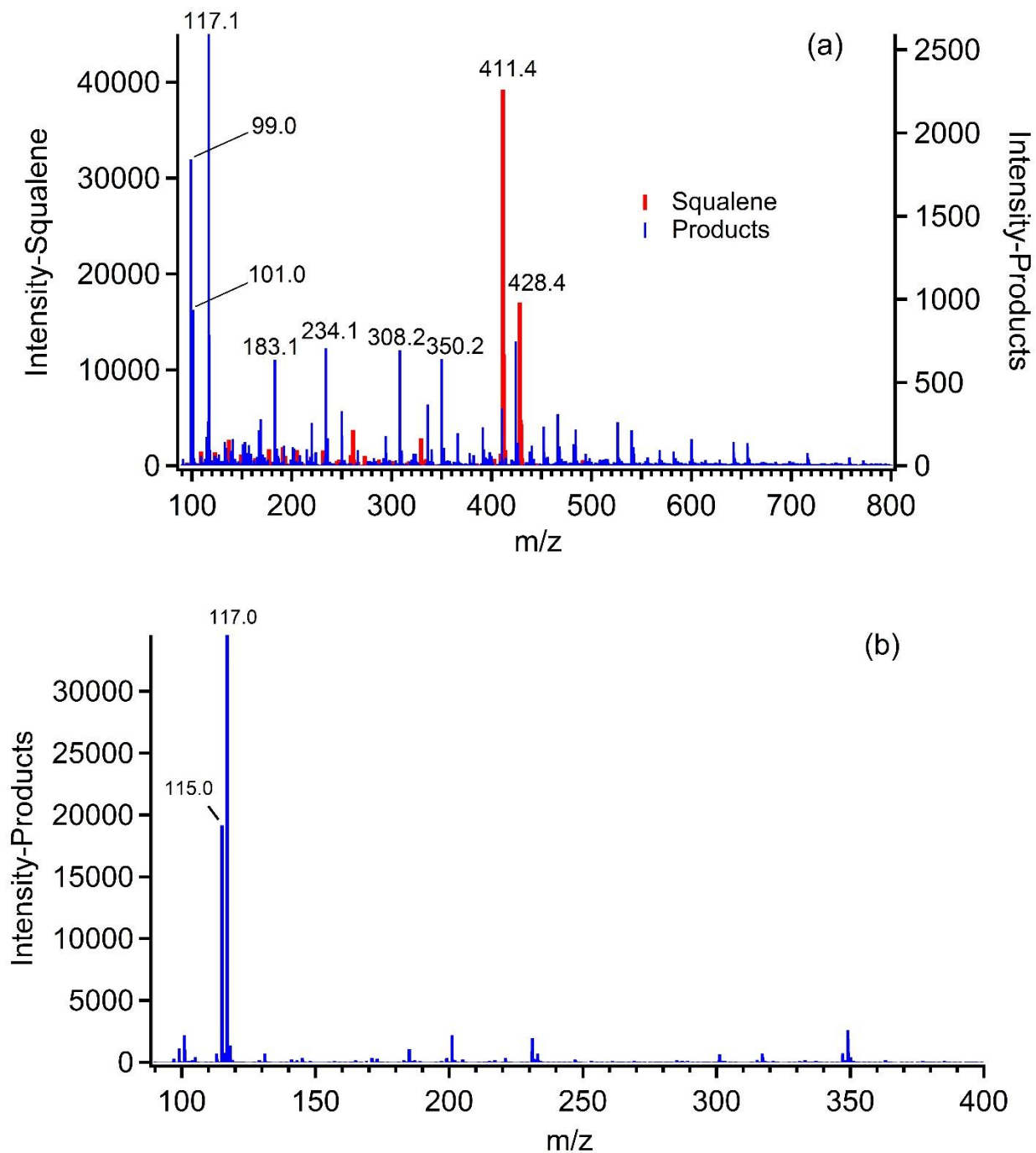


Figure S1. Mass spectrum (red) of squalene obtained under positive (a) and negative (b) modes. The blue trace is the product difference mass spectrum, i.e. it is the mass spectrum formed by subtracting that observed of pure squalene from that observed after squalene is exposed to ozone at 50 ppb for 90 minutes. Note the different scales on the y-axes in (a).

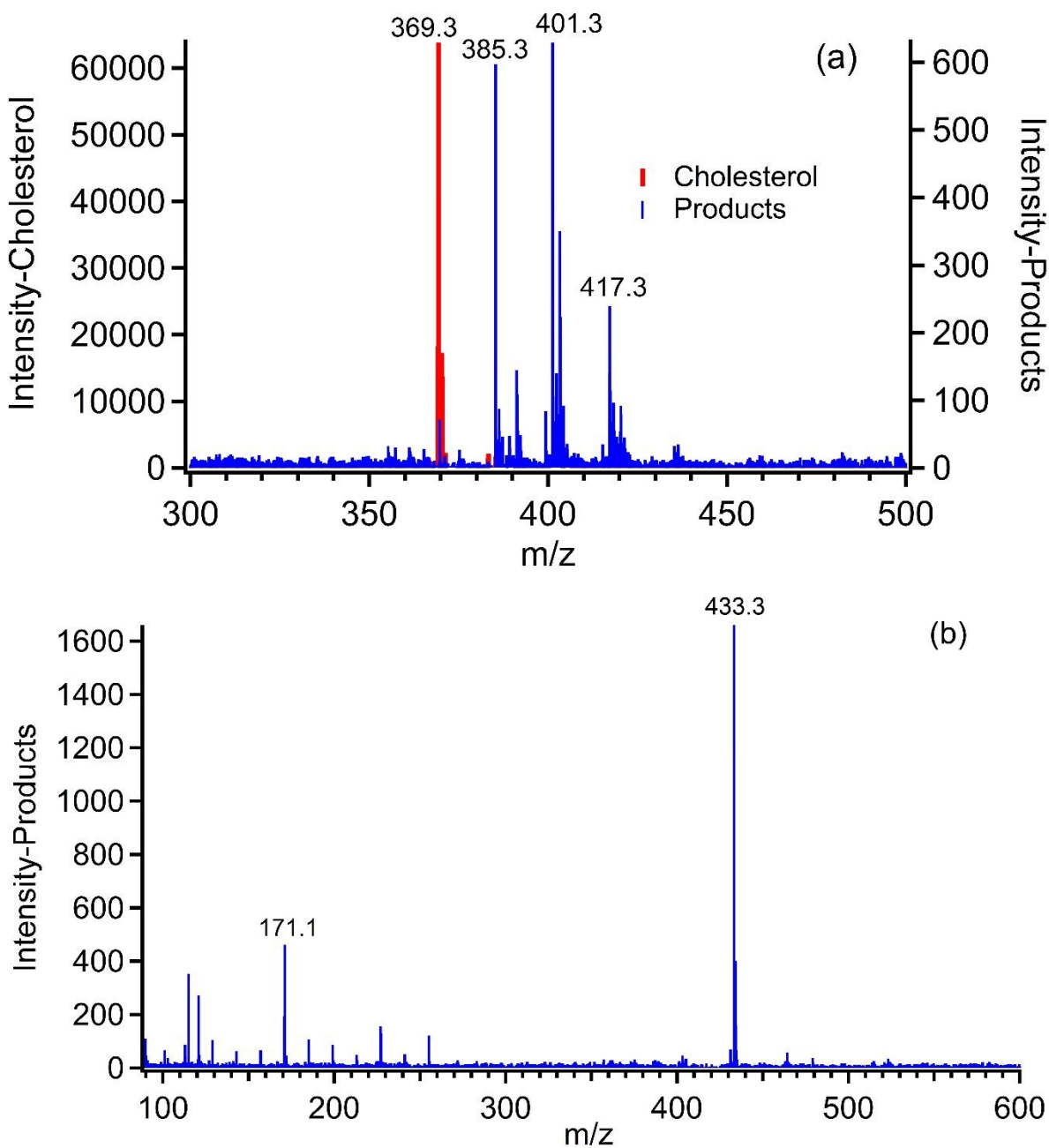


Figure S2. Mass spectrum (red) of cholesterol obtained under positive (a) and negative (b) modes. The blue trace is the product difference mass spectrum, i.e. it is the mass spectrum formed by subtracting that observed of pure cholesterol from that observed after squalene is exposed to ozone at 50 ppb for 90 minutes. Note the different scales on the y-axes in (a).

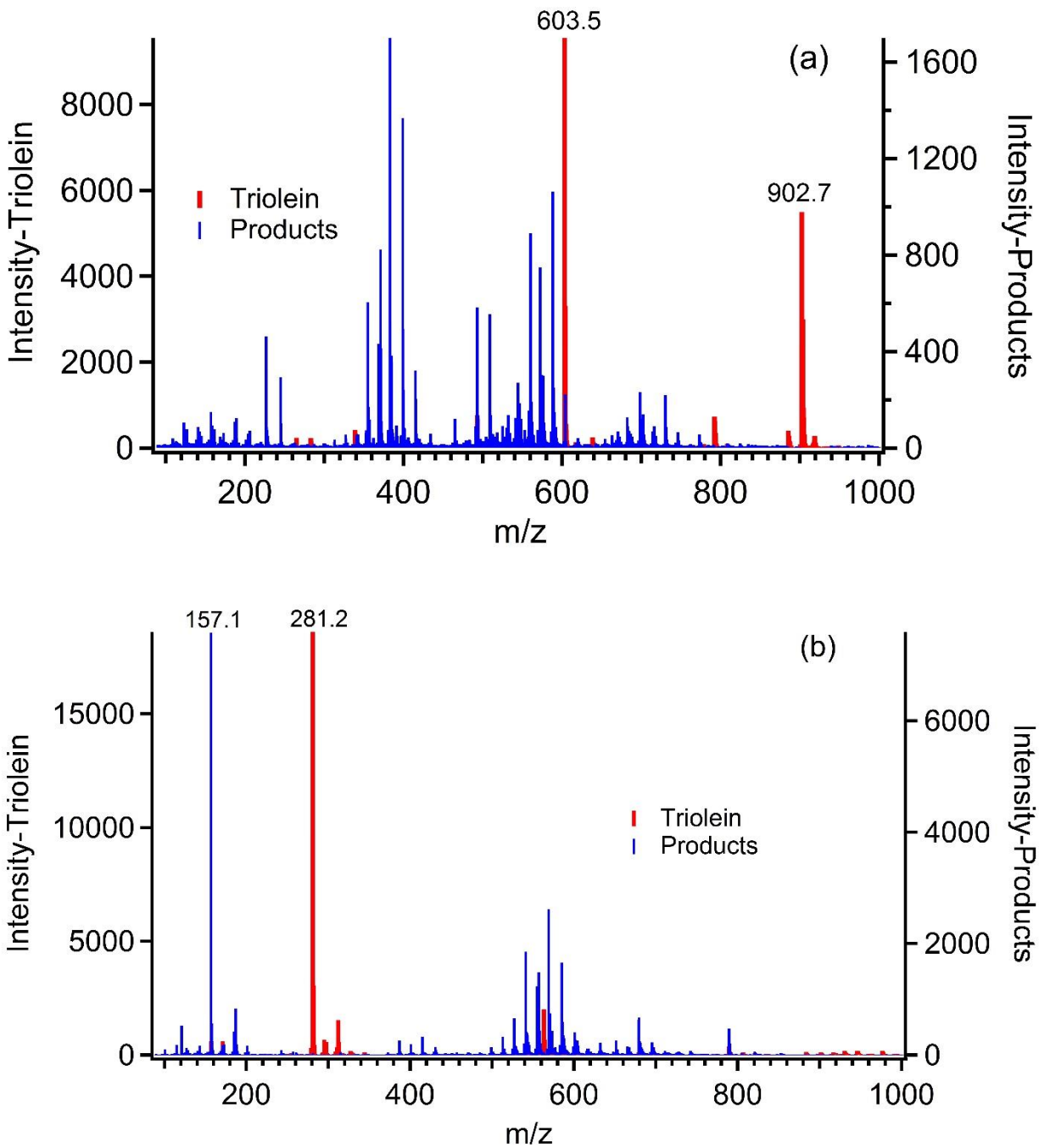


Figure S3. Mass spectrum (red) of triolein obtained under positive (a) and negative (b) modes. The blue trace is the product difference mass spectrum, i.e. it is the mass spectrum formed by subtracting that observed of pure triolein from that observed after squalene is exposed to ozone at 50 ppb for 90 minutes. Note the different scales on the y-axes in (a).

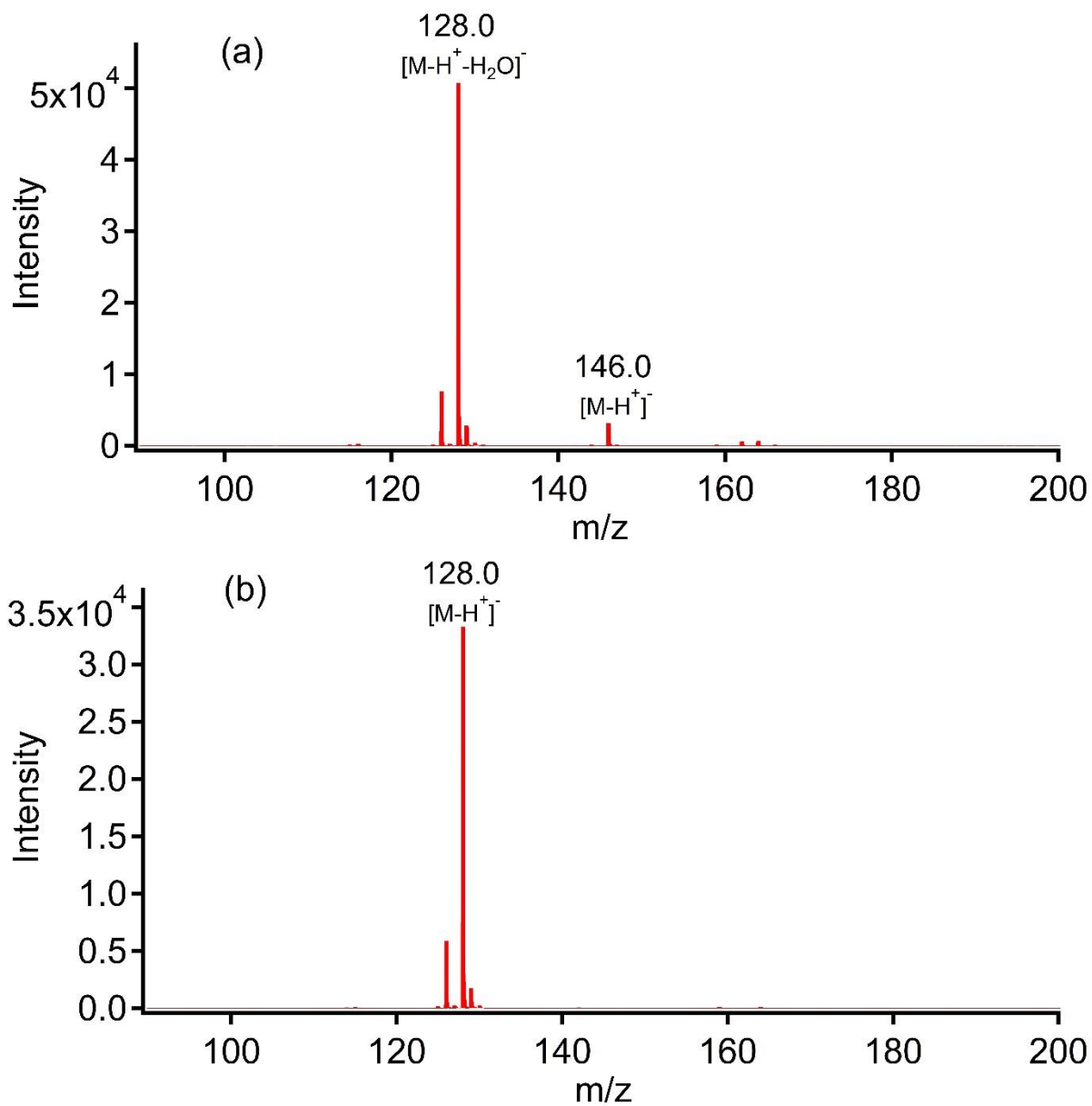


Figure S4. Mass spectrum of glutamic (a) and pyroglutamic acid (b) measured by DART-MS under negative mode. For glutamic acid m/z 146 and 128 (a) are due to $[M-H^+]^-$ and $[M-H^+-H_2O]^-$, respectively; for pyroglutamic acid (b) m/z 128 is due to $[M-H^+]^-$.

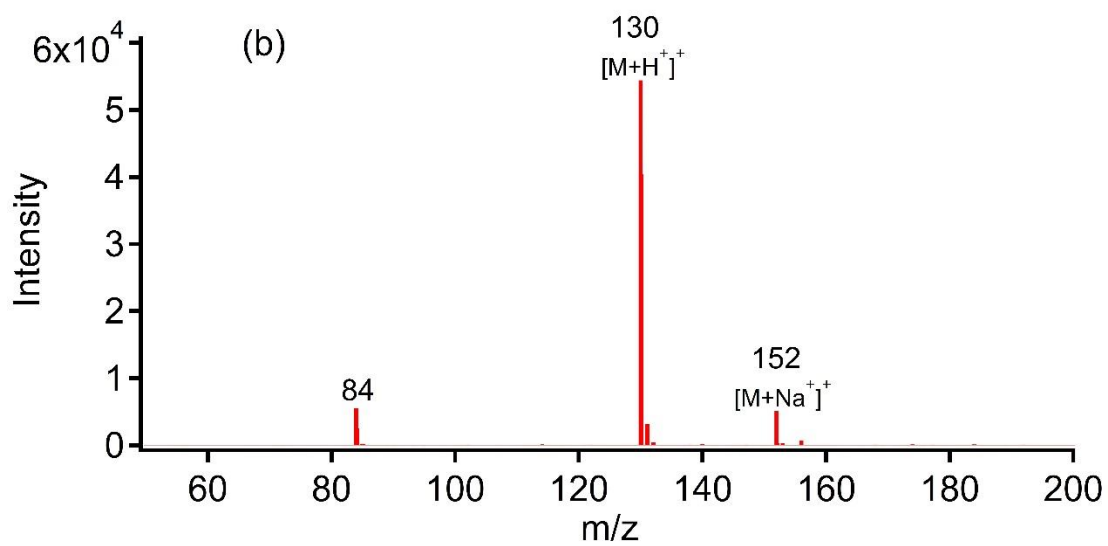
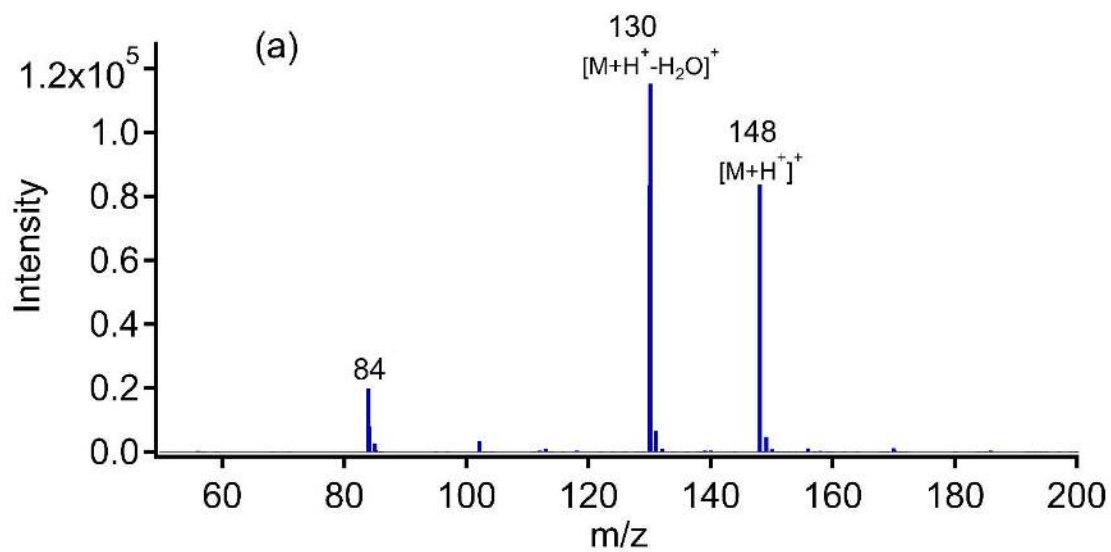


Figure S5. Mass spectra of glutamic acid (a) and pyroglutamic acid (b) obtained by the ESI-MS under positive mode.

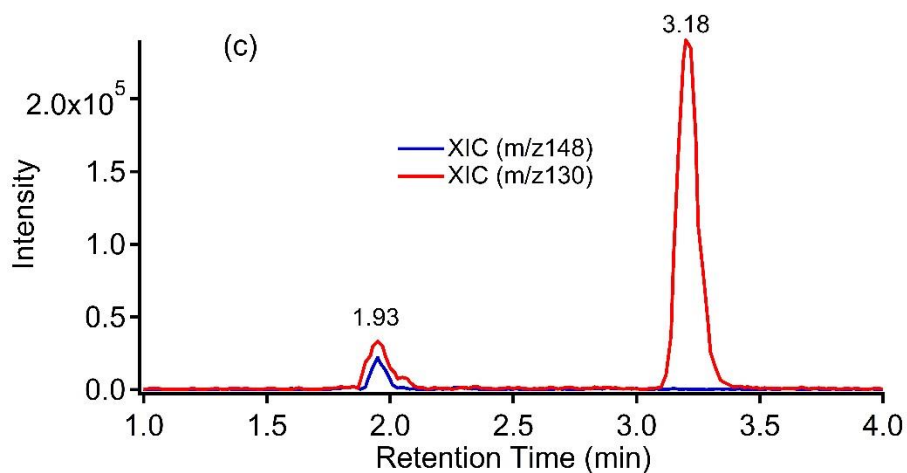
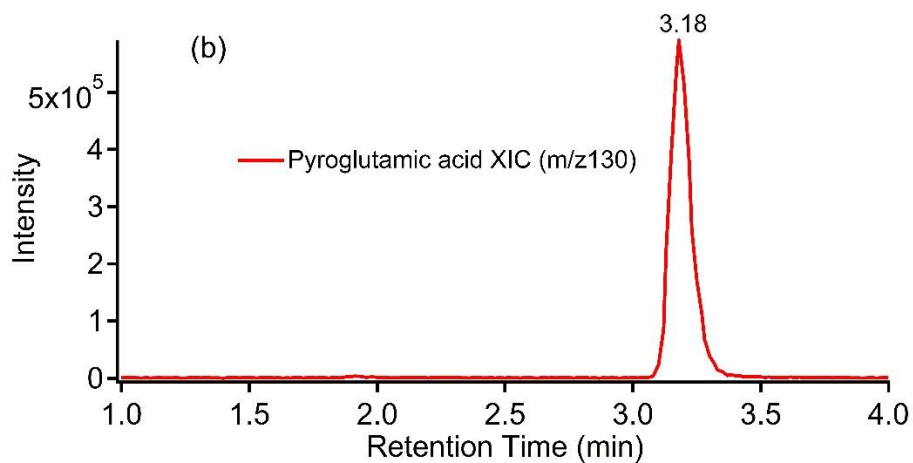
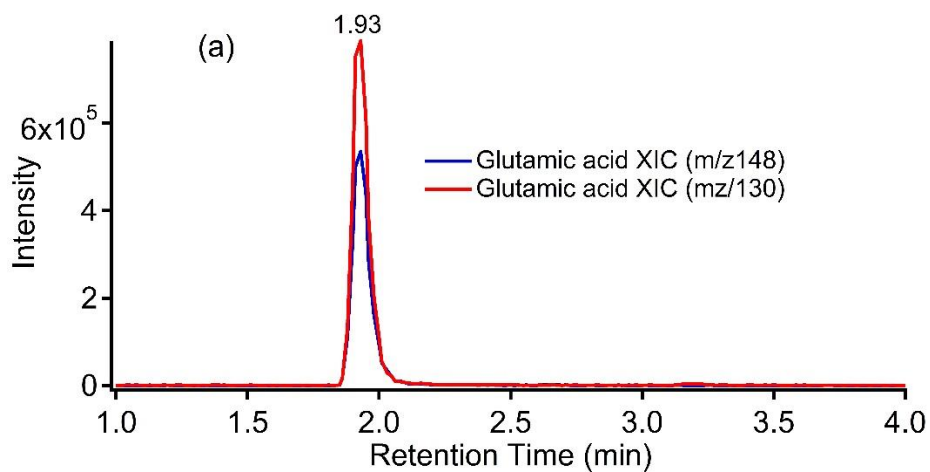


Figure S6. Extracted ion chromatogram (i.e. mass spectral intensity at the indicated mass-to-charge ratio) as a function of retention time) for the HPLC-MS analysis of (a) glutamic acid, (b) pyroglutamic acid and (c) aqueous extract of skin oils (see SI-Text for explanation).

Table S1. Major peaks of the un-oxidized and oxidized skin oil DART-MS spectra

	Un-oxidized	Oxidized
Positive mode	130.0, 311.1, 369.3, 411.4, 428.4, 451.4, 465.4, 479.4, 493.5, 507.5, 521.4, 523.4, 533.5, 535.5, 537.4, 547.4, 549.5, 550.5, 551.5, 563.5, 565.3, 575.4, 577.5, 579.5, 806.6, 808.7, 820.7, 822.7, 834.7, 836.8, 846.7, 848.7	101.0, 117.0, 130.0, 130.0, 311.1, 369.3, 383.3, 425.3, 441.3, 453.3, 455.3, 467.4, 469.3, 474.3, 523.4, 530.4, 537.4, 544.4, 551.5, 555.8, 565.5, 572.4, 586.4, 588.4, 616.4, 684.5, 686.5, 728.5
Negative mode	90.0, 137.0, 154.1, 227.2, 253.2, 255.2, 281.2, 405.0, 537.5, 798.7	90.0, 115.0, 117.0, 137.0, 145.0, 187.1, 255.2, 405.0, 457.3, 571.4, 585.4, 599.4, 613.4, 731.5, 798.7

Table S2. Major peaks of squalene and its ozonolysis products obtained by DART-MS

	Reactants	Products
Positive mode	411.4, 428.4	99.0, 101.0, 117.1, 183.1, 234.1, 308.2, 350.2, 424.2, 452.2, 466.3, 484.3, 526.2, 540.3
Negative mode	None	101.0, 115.0, 117.0, 201.1, 231.1, 349.1

Table S3. Major peaks of cholesterol and its ozonolysis products obtained by DART-MS

	Reactants	Products
Positive mode	369.3	385.3, 391.3, 401.3, 403.3, 417.3
Negative mode	None	115.0, 121.0, 171.1, 433.3

Table S4. Major peaks of triolein and its ozonolysis products obtained by DART-MS

	Reactants	Products
Positive mode	603.5, 902.7	227.1, 245.1, 355.2, 371.2, 383.2, 399.2, 415.2, 493.3, 509.3, 544.3, 560.3, 572.3, 588.3, 682.5, 698.5, 730.4
Negative mode	281.2, 563.5	157.1, 187.1, 527.3, 541.3, 557.3, 569.3, 585.3, 679.4, 789.6

SI – Text

HPLC-ESI-MS Analysis of Glutamic and Pyroglutamic Acids in Skin Oil:

Kimwipes were used to collect skin oils from the participant. The Kimwipes were cleaned by sonication with 20mL dichloromethane for 15 minutes followed by 15 minutes sonication with 20mL methanol and then drying under nitrogen. The skin oils were collected by wiping the participant's face and arms with the Kimwipes that were then extracted by sonication with 20 mL Milli-Q water. The aqueous extract was directly injected into an HPLC-ESI-MS (Agilent 1260 Infinity binary HPLC coupled to Agilent 6538 UHD quadrupole time-of-flight mass spectrometer) for analysis. The standards were prepared by dissolving the glutamic and pyroglutamic acids in Milli-Q water. Blank samples were extracted and analyzed in an analogous manner as the skin oil samples.

Figure S5 shows the mass spectra of glutamic (a) and pyroglutamic acid (b) obtained by ESI-MS in the positive ion mode. Figure S6 shows the extracted ion chromatograms of the HPLC-MS analysis of glutamic acid standard (~0.1mM) (a), pyroglutamic acid standard (~0.1mM) (b) and the aqueous extract of the skin oil (c). The HPLC separation was made using a 100 mm × 4.6 mm Gemeni NX 5µm C18 column (Phenomenex, Torrance, CA) and mobile phase consisting of 0.1% formic acid in water (A) and acetonitrile (B) at a flow rate of 0.5 mL/min. The mobile phase gradients were as follows: 0 min 5% B-1 min 5% B-11 min 95% B-11.01 min 95% B-14 min 100% B-14.01 min 5% B-15 min 5% B.